



Dose Reduction and Low-Contrast Detectability Using Iterative CBCT Reconstruction Algorithm for Radiotherapy

Technology in Cancer Research & Treatment
Volume 21: 1–9
© The Author(s) 2022
Article reuse guidelines:
sagepub.com/journals-permissions
DOI: 10.1177/15330338211067312
journals.sagepub.com/home/tct


Hayate Washio, BS^{1,2}, Shingo Ohira, PhD¹ ,
Yoshinori Funama, PhD³, Yoshihiro Ueda, MS¹,
Masahiro Morimoto, MD, PhD¹, Naoyuki Kanayama, MD, PhD¹,
Masaru Isono, MS¹, Shoki Inui, MS^{1,4}, Yuya Nitta, BS¹,
Masayoshi Miyazaki, BS¹, and Teruki Teshima, MD, PhD⁵

Abstract

Introduction: Several studies have reported the relation between the imaging dose and secondary cancer risk and have emphasized the need to minimize the additional imaging dose as low as reasonably achievable. The iterative cone-beam computed tomography (iCBCT) algorithm can improve the image quality by utilizing scatter correction and statistical reconstruction. We investigate the use of a novel iCBCT reconstruction algorithm to reduce the patient dose while maintaining low-contrast detectability and registration accuracy. **Methods:** Catphan and anthropomorphic phantoms were analyzed. All CBCT images were acquired with varying dose levels and reconstructed with a Feldkamp–Davis–Kress algorithm-based CBCT (FDK-CBCT) and iCBCT. The low-contrast detectability was subjectively assessed using a 9-point scale by 4 reviewers and objectively assessed using structure similarity index (SSIM). The soft tissue-based registration error was analyzed for each dose level and reconstruction technique. **Results:** The results of subjective low-contrast detectability found that the iCBCT acquired at two-thirds of a dose was superior to the FDK-CBCT acquired at a full dose (6.4 vs 5.4). Relative to FDK-CBCT acquired at full dose, SSIM was higher for iCBCT acquired at one-sixth dose in head and head and neck region while equivalent with iCBCT acquired at two-thirds dose in pelvis region. The soft tissue-based registration was 2.2 and 0.6 mm for FDK-CBCT and iCBCT, respectively. **Conclusion:** Use of iCBCT reconstruction algorithm can generally reduce the patient dose by approximately two-thirds compared to conventional reconstruction methods while maintaining low-contrast detectability and accuracy of registration.

Keywords

iterative CBCT, dose reduction, low-contrast detectability, registration error, radiotherapy

Abbreviations

CBCT, cone-beam computed tomography; iCBCT, iterative CBCT; SSIM, structure similarity index; FDK-CBCT, Feldkamp–Davis–Kress algorithm-based CBCT; OAR, organs at risk; CTS, CT scatter correction; SNR, signal-to-noise ratio; IR, iterative reconstruction; CNR, contrast-to-noise ratio; ROI, regions of interest; SD, standard deviation; HN, head and neck;

¹ Department of Radiation Oncology, Osaka International Cancer Institute, Osaka, Japan

² Graduate School of Health Sciences, Kumamoto University, Kumamoto, Japan

³ Department of Medical Radiation Sciences, Faculty of Life Sciences, Kumamoto University, Kumamoto, Japan

⁴ Department of Medical Physics and Engineering, Osaka University Graduate School of Medicine, Suita, Japan

⁵ Osaka Heavy Iron Therapy Center, Osaka, Japan

Corresponding Author:

Shingo Ohira, PhD, Osaka International Cancer Institute, 3-1-69 Otemae, Chuo-ku, Osaka, 541-8567, Japan.

Email: ueyama-si@mc.pref.osaka.jp



CTDI vol, computed tomography dose index volume; VMI, virtual monochromatic image; ASiR, adaptive statistical reconstruction; PTV, planning target volume.

Received: July 30, 2021; Revised: November 13, 2021; Accepted: November 30, 2021.

Introduction

Intensity-modulated radiotherapy and volumetric modulated arc therapy have rapidly been adopted as the standard of radiation therapy; these techniques enable highly conformal dose delivery to the target while minimizing the radiation dose to organs at risks (OARs).^{1,2} The safety and efficacy of these high precision irradiation techniques can only be assured when the patient or target position is the same as that of the planning computed tomography (CT). Cone-beam CT (CBCT) can provide volumetric information of patient anatomy and reduce setup errors using a 3D matching technique with an original planning CT.^{3,4} In addition, CBCT images can observe daily anatomical valuations, such as body weight loss, the shrinking of a tumor, and shifting of normal tissue, which are not visible for 2D images.

Repeated CBCT acquisition for the correction of patient setup error also results in additional radiation exposure to the patient. Therapeutic radiation adopts a highly modulated dose distribution; however, the CBCT dose distribution passes through the broad region of the body, including OARs. Several studies have reported the relation between the imaging dose and secondary cancer risk and have emphasized the need to minimize the additional imaging dose as low as reasonably achievable.^{5,6} Various trials have been conducted to reduce patients' exposure during imaging.^{7–14} Li et al.¹¹ have attempted to reduce the dose using a fan-beam collimator by changing the amount of x-ray blocked by the collimators and blocking pattern. They reported a 50% dose reduction and scatter reduction; however, they also warned of the potential of dosimetry inconsistency, penumbra, and a severe beam-hardening phenomenon caused by applying the fan-beam collimator to CBCT.

Recently, the iterative CBCT (iCBCT) reconstruction algorithm was introduced to clinical practice.¹⁵ By utilizing Acuros CT scatter correction (CTS) and statistical reconstruction, the iCBCT reconstruction algorithm enables the enhancement of image quality by increasing the signal-to-noise ratio (SNR) and reducing the streak and metal artifacts and image noises without a significant increase in the reconstruction time.^{15–17} However, assessments of the SNR, noise, and high-contrast resolution generally overestimate the performance of iterative reconstruction (IR), whereas the low-contrast resolution can be degraded by IR.^{18,19} Low-contrast resolution is required for soft tissue matching registration and observing the daily change of anatomy compared with high-contrast resolution. Although sufficient high-contrast resolution for bone matching may be achieved using low-dose CBCT, the effect of dose reduction on low-contrast detectability should be carefully examined. To the best of our knowledge, there are no previous studies that evaluate whether iCBCT can reduce the patient dose while maintaining low-contrast detectability and registration accuracy.

The aim of this study is to evaluate the feasibility of the iCBCT reconstruction algorithm compared with the conventional method. The evaluation determined whether the iCBCT reconstruction algorithm can reduce the patient dose while maintaining low-contrast detectability and registration accuracy. The low-contrast detectability was evaluated subjectively by reviewers and objectively using a structure similarity index (SSIM).

Methods

Catphan Phantom Study

Approval from an ethics committee is not required for this study because only phantoms were used for the experiments.

The CTP 730 module of the Catphan 604 phantom (The Phantom Laboratory) (20 cm in diameter) was used for the subjective and contrast-to-noise ratio (CNR) assessments. CBCT scans were performed using a gantry-mounted onboard imager on a Truebeam accelerator (Varian Medical Systems). The acquisition parameters are shown in Table 1. The full-dose acquisition parameters were determined in accordance with the patient protocol of our institute for head stereotactic irradiation. These parameters were vendor-provided values. All acquisitions were repeated 3 times to compensate random errors in date measurements. Two CBCT images, a conventional Feldkamp–Davis–Kress algorithm-based CBCT (FDK-CBCT), and an iCBCT, were reconstructed from the same raw CBCT dataset. The default FDK reconstruction included a kernel-based scatter correction, beam hardening correction, Hounsfield unit conversion, and ring correction.²⁰ In addition to this default reconstruction, iCBCT employs Acuros CTS and statistical analysis, and it enables a more efficient scatter correction while preserving structure edges. The details of the iCBCT reconstruction algorithm were described in our previous study.¹⁷ The iCBCT reconstruction has a peculiar adjustable factor called the noise suppression factor, which has 5 levels (very low to very high). The noise suppression factor controls the amount of noise in an image; however, there is a risk of generating over-smoothed images with a high noise suppression factor.¹⁵ Thus, we used a noise suppression factor of modest strength (medium) in this study. The standard reconstruction filter was used for both the FDK and iCBCT reconstruction.

Subjective Evaluation. A subjective evaluation was performed in a randomized and blind procedure by 2 radiation oncologists and 4 medical physicists with 18, 12, 11, 11, 7, and 6 years of experience in reviewing images and contouring structures. The 1% contrast rods in the CTP 730 module of the Catphan 604 phantom have different diameters (2–15 mm) and were assigned numbers from largest to smallest diameter (Figure 1). The subjective low-contrast detectability was rated based on the smallest detected rod number. A high score

Table 1. Acquisition Parameters of CBCT.

Parameters	Anthropomorphic phantom														
	Catphan phantom			Head				Head and Neck				Pelvis			
	Full	2/3	1/3	Full	2/3	1/3	1/6	Full	2/3	1/3	1/6	Full	2/3	1/3	1/6
Reconstruction method	FDK, iCBCT			FDK, iCBCT				FDK, iCBCT				FDK, iCBCT			
Tube voltage (kVp)	100			100				100				125			
Tube current (mA)	80	52	26	80	52	26	13	30	20	10	5	75	50	25	
Exposure (mAs)	1200	780	390	1200	780	390	195	300	200	100	50	1350	900	450	225
CTDI (mGy)	25.3	16.5	8.2	25.3	16.5	8.2	4.1	6.3	4.2	2.1	1.1	20	13.3	6.7	3.3
Bow tie filter	Half fan			Half fan				Full fan				Half fan			
Acquisition arc	Full-rotation			Full-rotation				Half-rotation				Full-rotation			
Gantry speed (deg/s)	5			5				6				6			

Abbreviations: FDK, Feldkamp–Davis–Kress; CBCT, cone-beam CT; iCBCT, iterative CBCT.

indicates that reviewers can detect small diameter rods, thereby inferring superior low-contrast detectability.

CNR. Circular regions of interest (ROIs), 10 mm in diameter, were placed in the center of the 15 mm 1% contrast rods and the center of phantom. These ROIs were relocated on iCBCT images. The mean HU value and standard deviation (SD) within these ROIs were recorded. CNR was calculated by using the formula,²¹

$$CNR = \frac{HU \text{ contrast} - HU \text{ background}}{SD \text{ background}}$$

Anthropomorphic Phantom Study

An anthropomorphic phantom (PH-47, Kyoto Kagaku) was used for the objective assessment. The phantom consisted of

human-mimicked tissues from head to femur. Because iCBCT reconstruction does not reduce motion artifacts, the vender recommends the use of iCBCT for regions where the motion artifacts are generally small. Thus, the scan acquisitions were conducted for 3 parts of the phantom: head, head and neck (HN), and pelvis. Fan-beam CT was performed on a fast kilovoltage-switching CT (Revolution HD, GE Healthcare) with switching tube voltages between 80 and 140 kVp. The scanning parameters of fan-beam CT are shown in Table 2. The CBCT images were acquired using 4 different dose levels: full-dose, two-thirds of a dose, one-third of a dose, and one-sixth of a dose. The full-dose acquisition parameters were determined in accordance with the patient protocols of our institute (Table 1). The reconstruction parameters of the CBCT were the same as those in the Catphan phantom study.

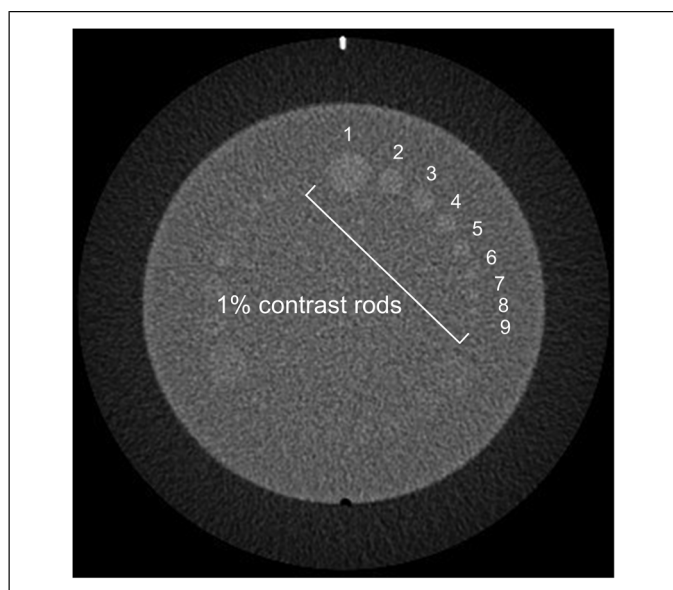


Figure 1. Axial image of the CTP 730 module of the Catphan 604 phantom acquired using a fan-beam CT. The 1% contrasts rods have different diameters (15–2 mm) and were assigned numbers from largest to smallest diameters. Window setting; level 40 HU, width 200 HU.

SSIM Analysis. The SSIM, which was developed by Wang et al.,²² was used for the objective low-contrast detectability analysis. The SSIM can predict image quality similarly to human visual perception by considering 3 aspects: luminescence, contrast, and structural similarity. The SSIM represents the similarity of 2 images using a scale of up to 1, where 1 denotes

Table 2. Acquisition Parameters of Fan-Beam CT.

Parameters	Head	Head and neck	Pelvis
Average tube current (mA)	550	375	375
CTDI vol (mGy)	105.5	15.0	12.9
Slice thickness (mm)	2	2	2
Iterative reconstruction level	ASiR-V 20%	-	ASiR 40%
Reconstruction filter	Standard	Standard	Standard
VMI energy level (keV)	77	77	77

Abbreviations: CTDI vol, computed tomography dose index volume; VMI, virtual monochromatic image; ASiR, adaptive statistical reconstruction.

completely the same image sets, and a score smaller than 1 denotes different image sets. The application of SSIM has been extended to the field of radiology.^{19,23–25} The SSIM was calculated for CBCT images, which were compared with reference fan-beam CT images by varying dose levels and reconstruction techniques. A 11×11 circular-symmetric Gaussian weighting function with SD of 1.5 samples was used to calculate local statistics. The calculation of the SSIM was conducted using plug-ins written for ImageJ software (<https://imagej.nih.gov/ij/>).

Registration Analysis. The registration accuracy was analyzed only for the pelvis phantom because the head and HN phantom used in this study hardly contained soft tissue or tumor-like structures. The pelvis phantom consisted of the pelvic bone, prostate, bladder, seminal vesicle, and rectum. The registration analysis was conducted as per the following steps: (i) Each CBCT image was matched with a reference fan-beam CT image by applying a ROI that covered the whole volume of the CBCT image and auto-registration process. This position was regarded as the default position. (ii) The image position was shifted 5 mm from the default position in the lateral, vertical, and longitudinal directions, respectively. (iii) 3D auto-registration was executed by varying the registration method; for bone-based registration, the ROI was set to cover the large part of the pelvic bone and not include the phantom's outer contour, and for soft tissue-based registration, the ROI was set to cover the prostate and not include any high-contrast objects, such as a bone. The ROI location for each registration method was shown in Figure 2. (iv) The variances from the default position were recorded as a registration error for each dose level, reconstruction technique, and ROI placement. The registration analysis was performed using commercial software (ARIA, Varian Medical Systems).

Statistical Analysis

SPSS version 24 (IBM Corp.) was used for the statistical analysis. The subjective low-contrast detectability score was visualized using box and whisker plots. The Wilcoxon signed-rank test was used to analyze the difference in the CBCT images compared with full-dose FDK-CBCT images. A P value $< .05$ was considered statistically significant.

Results

Catphan Phantom Study

Subjective Evaluation. Figure 3 shows the Catphan phantom images at each dose level and reconstruction technique. The low-contrast detectability decreases with a decreasing dose level for both the FDK-CBCT and iCBCT images (Figure 4).

The iCBCT images obtain high subjective scores compared with the FDK-CBCT images acquired at the same dose level; however, a significant difference is not obtained for a one-third

dose level (FDK-CBCT vs iCBCT, 2.3 vs 2.9 [$P = .07$] for one-third dose, 3.4 vs 6.4 [$P < .05$] for two-thirds dose, 5.4 vs 7.7 [$P < .05$] for full dose). Moreover, a reduction to a two-thirds dose level for iCBCT results in better image quality compared to an FDK-CBCT acquired at a full dose ($P < .05$). When dose reduction is significant, the iCBCT images result in significant degradation of low-contrast detectability and are inferior compared to FDK-CBCT acquired at the full-dose level ($P < .05$). The best score is 7.7, which is for iCBCT images acquired at full dose, whereas the worst score is 2.3 for FDK-CBCT acquired at a one-third dose level.

CNR. The mean HU value, SD value, and CNR for each reconstruction method and dose level are summarized in Table 3. The SD value increases and CNR decreases with a decreasing dose level. The iCBCT images show higher CNR compared to FDK-CBCT images (0.03-0.11 for FDK-CBCT, 0.10-0.15 for iCBCT).

Anthropomorphic Phantom Study

SSIM Analysis. Figure 5 shows the SSIM between CBCT images acquired at varying dose levels, reconstruction techniques, and acquisition regions and a reference fan-beam CT. Figure 6 shows CBCT images acquired at one-sixth of a dose and full dose and reference fan-beam CT images for the (a) head, (b) HN, and (c) pelvis. The SSIM shows that the image quality, especially low-contrast detectability, decreases with a decreasing dose for both reconstruction techniques and all acquisition regions.

For each acquisition region, the iCBCT images acquired at the full dose exhibit the best score (0.68, 0.74, and 0.66 for head, HN, and pelvis, respectively). The worst score is observed for FDK-CBCT acquired at one-sixth of a dose (0.56, 0.58, and 0.46 for head, HN, and pelvis, respectively). SSIMs of iCBCT acquired at a one-sixth dose are better than the FDK-CBCT acquired at a full dose for the head and HN regions (full-dose FDK-CBCT vs one-sixth dose iCBCT, 0.60 vs 0.63 for head, 0.64 vs 0.68 for HN). However, for the pelvis, a one-sixth dose iCBCT is inferior to the one-third, two-thirds, and full-dose FDK-CBCT, and the one-third dose iCBCT shows similarity to the full-dose FDK-CBCT (0.62 and 0.63, respectively).

Registration Analysis. Table 4 shows the registration errors at each dose level, reconstruction technique, and registration method. The bone-based method indicates accurate registration, and the registration errors are less than 0.2 mm regardless of dose level and reconstruction technique. The registration errors slightly increase for the soft tissue-based method compared with the bone-based method. The registration errors are less than 0.6 mm with the exception of the one-sixth dose FDK-CBCT, which exhibits errors of 2.2 and 1.5 mm in the lateral and vertical directions, respectively.

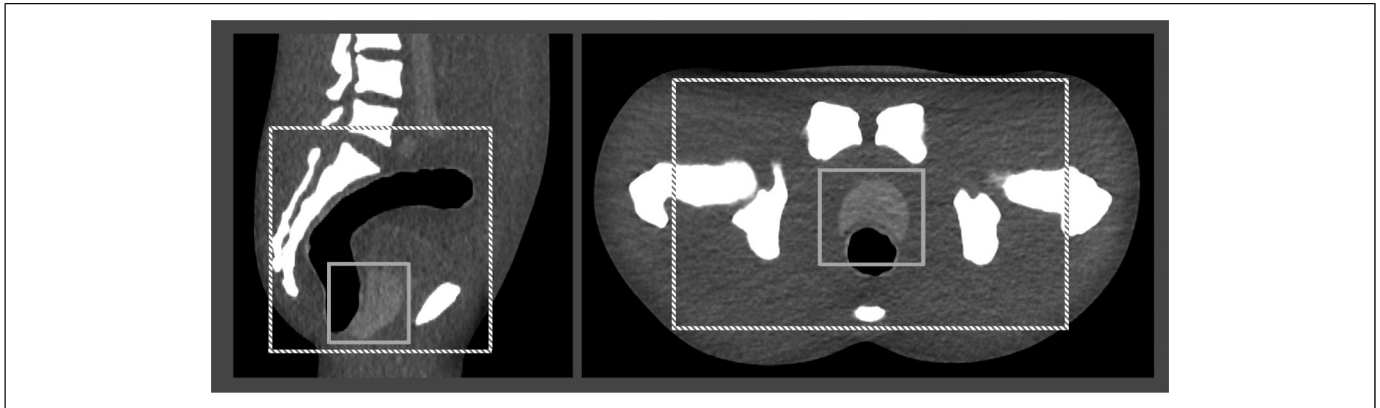


Figure 2. Sagittal and axial images of an anthropomorphic phantom acquired by using fan-beam CT. The green and red regions denote the ROI location for soft tissue-based and bone-based method, respectively. Window setting; level 50 HU, width 300 HU. ROI: region of interest.

Discussion

CBCT registration significantly contributes to radiotherapy by observing anatomical valuations and reducing positioning uncertainty and planning target volume (PTV) margins, which can reduce the severity of radiation-related toxicity.^{4,26} The recently-introduced iCBCT reconstruction algorithm is increasingly implemented in clinical practice, and its feasibility has been reported in several studies.^{15,16} However, there are no studies that focus on the feasibility of utilizing iCBCT for effective dose reduction while maintaining low-contrast detectability and registration accuracy. The reduction of the patient dose for image-guided radiotherapy raises increasing concern. Ding

et al.²⁷ enhanced the importance of minimizing and managing the imaging dose while improving treatment delivery. Compared with the dose reduction method that is typically used,^{11–14} iCBCT does not require additional manual work, high computational power, and considerable reconstruction time. The additional reconstruction time from conventional method was approximately 20 s for HN patients.¹⁷

Conventional objective image analyses, such as the SNR, noise power spectrum, and transfer functions, are unsuitable for the evaluation of the IR algorithm because it does not fulfill the condition of a shift-invariant linear imaging system.^{18,19} Hence, McCollough et al.²⁸ recommended subjective analysis as a low-contrast detectability evaluation for the IR algorithm instead of the conventional reconstruction method. They conducted image reviews of 4 6 mm low-contrast rods in an accreditation phantom by 3 viewers and reported effective dose reduction using IR for diagnostic fan-beam CT. In

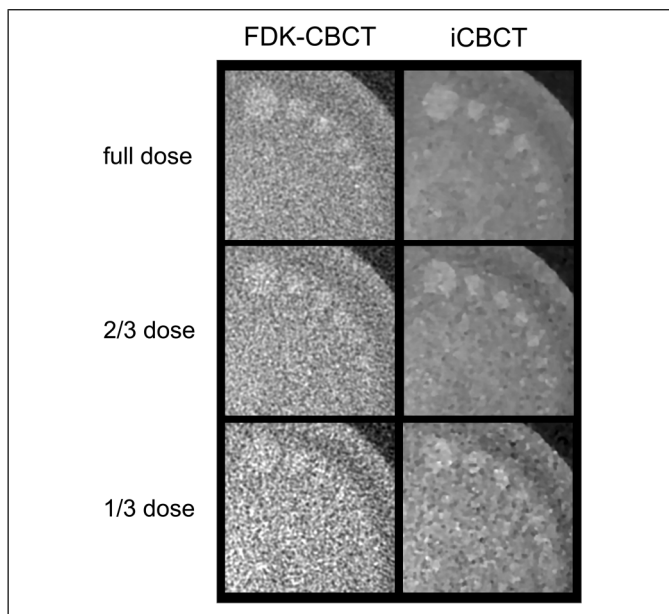


Figure 3. Example CT images of low-contrast rods in the CTP 730 module acquired using FDK-CBCT and iCBCT. Acquisitions were repeated 3 times at each dose level. Window setting; level 40 HU, width 200 HU. FDK, Feldkamp–Davis–Kress; CBCT, cone-beam CT; iCBCT, iterative CBCT.

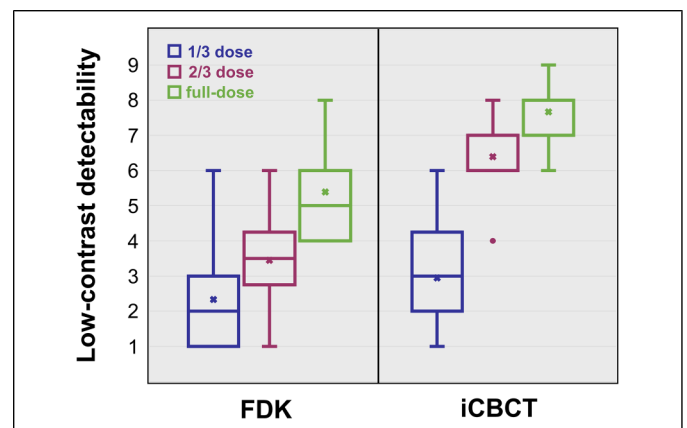


Figure 4. Low-contrast detectability score of subjective analysis for each dose level and reconstruction technique. The low-contrast detectability is decreased for decreasing dose levels for both the FDK-CBCT and iCBCT images. A two-thirds dose reduction for iCBCT produces better image quality compared to FDK-CBCT acquired at full-dose. FDK, Feldkamp–Davis–Kress; CBCT, cone-beam CT; iCBCT, iterative CBCT.

Table 3. Mean HU Value, SD Value, and CNR for Each Reconstruction Method and Dose Level.

Parameters		1% contrast rod		Background		CNR
		HU value	SD value	HU value	SD value	
FDK	Full-dose	52.7 ± 0.5	65.6 ± 4.9	47.0 ± 0.8	65.0 ± 0.4	0.09
	2/3 dose	52.3 ± 2.5	71.1 ± 0.2	45.0 ± 4.5	66.2 ± 0.4	0.11
	1/3 dose	45.0 ± 3.5	74.2 ± 1.4	42.3 ± 4.0	71.5 ± 0.5	0.03
iCBCT	Full-dose	57.0 ± 0.8	61.9 ± 0.5	48.3 ± 0.5	56.6 ± 0.2	0.15
	2/3 dose	54.3 ± 1.7	62.0 ± 0.3	46.0 ± 2.1	56.8 ± 0.4	0.15
	1/3 dose	49.7 ± 1.7	65.8 ± 1.9	43.3 ± 3.7	62.1 ± 0.6	0.10

Abbreviations: FDK, Feldkamp–Davis–Kress; CBCT, cone-beam CT; iCBCT, iterative CBCT; CNR, contrast-to-noise ratio.

accordance with their method, we conducted subjective analysis using the low-contrast module of the Catphan phantom. By scoring the smallest detected 1% contrast rod number, we observed that the low-contrast detectability of iCBCT acquired at two-thirds of a dose was superior to that of FDK acquired at a full dose. The low-dose reconstruction generates noisy and artifact-induced images in accordance with the trade-off between the dose level and image quality; however, the iCBCT algorithm can maintain image quality for a moderate dose reduction by utilizing scatter correction and edge preservation.

We additionally evaluated the low-contrast detectability objectively using an anthropomorphic phantom that reproduced a structured background, such as a human tissue, in contrast to the Catphan phantom. We applied the SSIM analysis, which can predict image quality similarly to human visual perception and represent low-contrast detectability. The results showed that similarity with the reference CT was higher for iCBCT acquired at one-sixth of a dose than for FDK acquired at a full dose in the head and HN regions. However, the SSIM result exhibited dramatic image quality degradation as the

dose decreased for both CBCT reconstruction techniques in the pelvis region. We assumed that iCBCT algorithm would not well work to reduce noise and artifact when image contains much scatters such as pelvic image acquired at low dose. To summarize the subjective and objective analysis, the iCBCT reconstruction algorithm can generally reduce the dose by approximately two-thirds and maintain low-contrast detectability compared with the FDK–CBCT. However, the effect of the dose reduction on image quality is different depending on the object sizes and required imaging tasks. In our study, substantial dose reduction is feasible for small objects, such as the head and HN regions; however, this is not suitable for large objects, such as the pelvis region. Thus, when introducing the IR algorithm to clinical practice and attempting to reduce the patient dose, we recommend that an assessment of the low-contrast detectability should be conducted on the specific imaging task reference of the routine dose setting of the institute.

We also examined the effect of dose reduction on the registration error for FDK–CBCT and iCBCT in the pelvis region. Bone-based matching was successfully performed with a

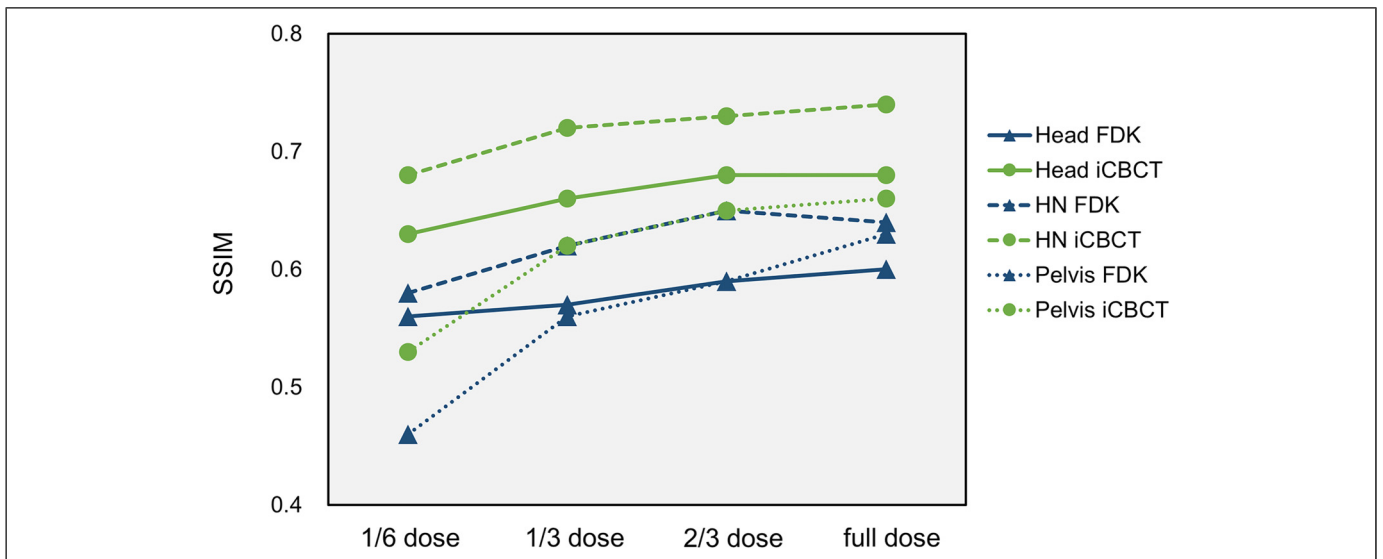


Figure 5. SSIM between CBCT images acquired at varying dose levels, reconstruction techniques, and acquisition regions and a reference fan-beam CT. SSIM, structure similarity index; FDK, Feldkamp–Davis–Kress; CBCT, cone-beam CT; iCBCT, iterative CBCT.

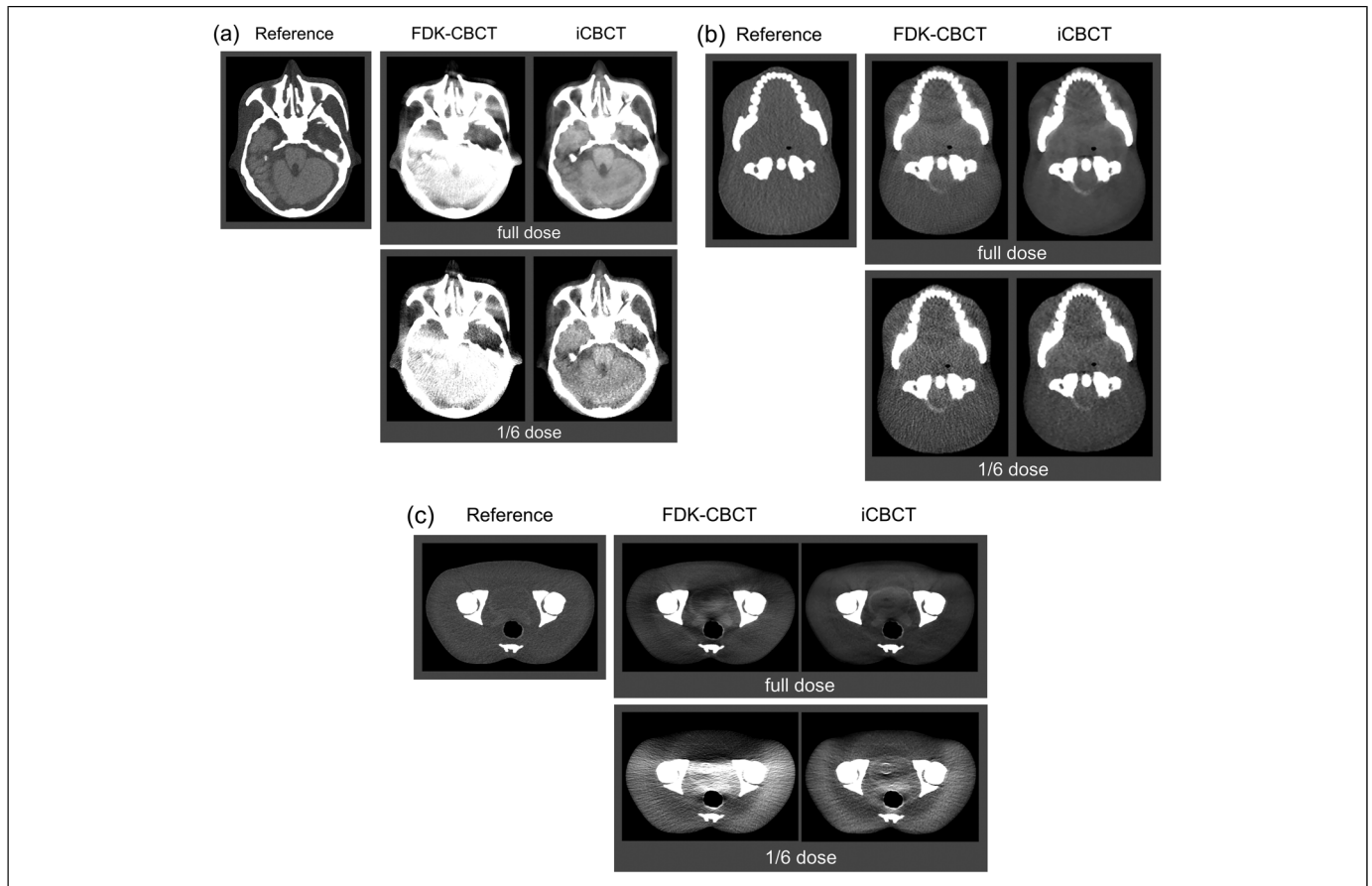


Figure 6. Axial CT images of anthropomorphic phantom for the (a) head, (b) head and neck, and (c) pelvis regions acquired with FDK-CBCT and iCBCT. Window setting: level 40 HU, width 200 HU (a), 40 HU, 300 HU (b); 50 HU, 300 HU (c). FDK, Feldkamp–Davis–Kress; CBCT, cone-beam CT; iCBCT, iterative CBCT.

registration error of less than 0.2 mm, regardless of imaging dose level. For soft tissue-based registration, the error was within 0.6 mm for iCBCT, whereas that for FDK-CBCT increased with decreasing dose levels; the maximum error was 2.2 mm. Although the registration error was within 3 to 8 mm, which was adopted as a PTV margin in several

institutes for prostate cancer,²⁹ the effect of dose reduction on soft tissue-based registration cannot be ignored when conducting radiotherapy within a tight margin. Loutfi-Krauss et al.³⁰ examined this relationship by applying a low-contrast structured phantom with a uniform background. They reported that low-contrast structure-based registration can be performed successfully, regardless of the imaging dose level and image quality. Considering the results of both our and their studies, the soft tissue-based registration may vary depending on imaging dose level and background structure. The target of the pelvis region is often surrounded by high- and low-contrast materials, such as pelvic bone and air in the rectum; therefore, we should be particularly careful for the dose setting and registration in this area.

This study has the following limitations. First, we evaluated the SSIM only for the head, HN, and pelvis regions. Although the iCBCT demonstrates its advantages for regions where the motion artifacts are generally small, dose reduction is also desirable for the thorax region, which contains important OARs, such as the lungs, esophagus, heart, and spine. If the motion artifact can be minimized, for example, by adopting respiratory-gated CBCT, dose reduction using iCBCT may also be applied to the thorax and other regions. Second, we conducted the registration analysis

Table 4. Registration Errors in Lateral/Vertical/Longitudinal Direction for Each Dose Level, Reconstruction Techniques, and Registration Method.

Dose level	Bone-based		Soft tissue-based	
	FDK	iCBCT	FDK	iCBCT
Full-dose	-0.1/-0.1/ -0.1	-0.1/-0.1/ -0.1	0.0/-0.4/ -0.2	0.0/-0.2/ -0.1
2/3 dose	0.0/-0.1/0.0	0.0/-0.1/ -0.1	0.0/-0.4/ -0.2	0.1/0.0/0.2
1/3 dose	0.0/-0.1/ -0.1	0.1/0.0/0.0	0.0/-0.6/ -0.3	0.0/-0.4/ 0.3
1/6 dose	0.1/-0.1/ -0.2	0.0/-0.1/ -0.1	2.2/-1.5/ 0.0	0.1/0.6/0.2

Abbreviations: FDK, Feldkamp–Davis–Kress; CBCT, cone-beam CT; iCBCT, iterative CBCT.

using an anthropomorphic phantom that did not completely model the human complex body. Anatomical variations and movement of organs were also not included. Third, we did not examine other metrics affected by the dose decrease, such as the accuracy of the CT number and the dose calculation based on CBCT, because the study focused on the effect on low-contrast detectability and registration accuracy using iCBCT. Further study regarding the relationship between the dose reduction and these metrics should be conducted for low-dose adaptive radiotherapy. Fourth, the subjective evaluation by radiologists and medical physicists were applied to the study. The large-scale studies using the mathematical model observer with the Hotelling observer and channelized Hotelling observer model may be required to validate our results in addition to human vision.

Conclusion

This study confirmed that iCBCT algorithm allows the patient dose reduction by utilizing scatter correction and statistical reconstruction. Approximately two-thirds dose reduction is capable while maintaining low-contrast detectability and the accuracy of registration. However, the effect of the dose reduction on image quality may vary depending on object sizes and the required image tasks. The results and evaluation methods of this study may be useful for institutes that intend to introduce IR in clinical practice and reduce patient doses.

Acknowledgments

We would like to thank Editage (www.editafe.com) for English language editing.

Ethical Statement

Our study did not require an ethical board approval because it did not contain human or animal trials.


Declaration of Conflicting Interests

The authors declared no potential conflicts of interest with respect to the research, authorship, and/or publication of this article.

Funding

The authors disclosed receipt of the following financial support for the research, authorship, and/or publication of this article: This study was supported by JSPS KAKENHI Grant (Grant-in-Aid for Young Scientists 19K17285).

ORCID iD

Shingo Ohira  <https://orcid.org/0000-0002-6170-1471>

References

- Veldeman L, Madani I, Hulstaert F, De Meerleer G, Mareel M, De Neve W. Evidence behind use of intensity-modulated radiotherapy: a systematic review of comparative clinical studies. *Lancet Oncol.* 2008;9(4):367-375.
- Teoh M, Clark CH, Wood K, Whitaker S, Nisbet A. Volumetric modulated arc therapy: a review of current literature and clinical use in practice. *Br J Radiol.* 2011;84(1007):967-996.
- Li H, Zhu XR, Zhang L, et al. Comparison of 2D radiographic images and 3D cone beam computed tomography for positioning head-and-neck radiotherapy patients. *Int J Radiat Oncol Biol Phys.* 2008;71(3):916-925.
- Den RB, Doemer A, Kubicek G, et al. Daily image guidance with cone-beam computed tomography for head-and-neck cancer intensity-modulated radiotherapy: a prospective study. *Int J Radiat Oncol Biol Phys.* 2010;76(5):1353-1359.
- Kim DW, Chung WK, Yoon M. Imaging doses and secondary cancer risk from kilovoltage cone-beam CT in radiation therapy. *Health Phys.* 2013;104(5):499-503.
- Dzierma Y, Mikulla K, Richter P, et al. Imaging dose and secondary cancer risk in image-guided radiotherapy of pediatric patients. *Radiat Oncol.* 2018;13(1):168.
- Cheng JC-H, Liang C-H, Wu J-K, et al. Evaluation of radiation dose and positioning accuracy on x-ray volume imaging system for image-guided radiotherapy. *Nuclear Inst Methods Phys Res Sect B, Beam Inter Mater Atoms.* 2008;266(10):2203-2206.
- Ding GX, Munro P, Pawlowski J, Malcolm A, Coffey CW. Reducing radiation exposure to patients from kV-CBCT imaging. *Radiother Oncol.* 2010;97(3):585-592.
- Yan H, Cervino L, Jia X, Jiang SB. A comprehensive study on the relationship between the image quality and imaging dose in low-dose cone beam CT. *Phys Med Biol.* 2012;57(7):2063-2080.
- Morrow NV, Lawton CA, Qi XS, Li XA. Impact of computed tomography image quality on image-guided radiation therapy based on soft tissue registration. *Int J Radiat Oncol Biol Phys.* 2012;82(5):e733-e738.
- Li T, Li X, Yang Y, Zhang Y, Heron DE, Huq MS. Simultaneous reduction of radiation dose and scatter for CBCT by using collimators. *Med Phys.* 2013;40(12):121913.
- Parsons D, Robar JL. An investigation of kV CBCT image quality and dose reduction for volume-of-interest imaging using dynamic collimation. *Med Phys.* 2015;42(9):5258-5269.
- Kamezawa H, Arimura H, Shirieda K, Kameda N, Ohki M. Feasibility of patient dose reduction based on various noise suppression filters for cone-beam computed tomography in an image-guided patient positioning system. *Phys Med Biol.* 2016;61(9):3609-3636.
- Son K, Chang J, Lee H, et al. Optimal dose reduction algorithm using an attenuation-based tube current modulation method for cone-beam CT imaging. *PLoS One.* 2018;13(2):e0192933.
- Mao W, Liu C, Gardner SJ, et al. Evaluation and clinical application of a commercially available iterative reconstruction algorithm for CBCT-based IGRT. *Technol Cancer Res Treat.* 2019;18(1533033818823054).
- Gardner SJ, Mao W, Liu C, et al. Improvements in CBCT image quality using a novel iterative reconstruction algorithm: a clinical evaluation. *Adv Radiat Oncol.* 2019;4(2):390-400.
- Washio H, Ohira S, Funama Y, et al. Metal artifact reduction using iterative CBCT reconstruction algorithm for head and neck radiation therapy: a phantom and clinical study. *Eur J Radiol.* 2020;132(109293):1-6.

18. Yu L, Vrieze TJ, Leng S, Fletcher JG, McCollough CH. Technical note: measuring contrast- and noise-dependent spatial resolution of an iterative reconstruction method in CT using ensemble averaging. *Med Phys*. 2015;42(5):2261-2267.
19. Joemai RMS, Geleijns J. Assessment of structural similarity in CT using filtered backprojection and iterative reconstruction: a phantom study with 3D printed lung vessels. *Br J Radiol*. 2017;90(1079):20160519.
20. Wang A, Maslowski A, Messmer P, et al. Acuros CTS: a fast, linear Boltzmann transport equation solver for computed tomography scatter - part II: system modeling, scatter correction, and optimization. *Med Phys*. 2018;45(5):1914-1925.
21. Mao W, Gardner SJ, Snyder KC, et al. On the improvement of CBCT image quality for soft tissue-based SRS localization. *J Appl Clin Med Phys*. 2018;19(6):177-184.
22. Wang Z, Bovik AC, Sheikh HR, Simoncelli EP. Image quality assessment: from error visibility to structural similarity. *IEEE Trans Image Process*. 2004;13(4):600-612.
23. Alikhani B, Werner M, Jamali L, Wacker F, Werncke T. Image quality performance of virtual single-source CT using dual-source computed tomography. *Acad Radiol*. 2019;26(8):1095-1101.
24. Oyama A, Kumagai S, Arai N, et al. Image quality improvement in cone-beam CT using the super-resolution technique. *J Radiat Res*. 2018;59(4):501-510.
25. Kim DS, Lee S, Kim TH, et al. A respiratory-guided 4D digital tomosynthesis. *Phys Med Biol*. 2018;63(24):245007.
26. Navran A, Heemsbergen W, Janssen T, et al. The impact of margin reduction on outcome and toxicity in head and neck cancer patients treated with image-guided volumetric modulated arc therapy (VMAT). *Radiother Oncol*. 2019;130:25-31.
27. Ding GX, Alaei P, Curran B, et al. Image guidance doses delivered during radiotherapy: quantification, management, and reduction: report of the AAPM therapy physics committee task group 180. *Med Phys*. 2018;45(5):e84-e99.
28. McCollough CH, Yu L, Kofler JM, et al. Degradation of CT Low-contrast spatial resolution Due to the Use of iterative reconstruction and reduced dose levels. *Radiology*. 2015;276(2):499-506.
29. Ueda Y, Fukunaga JI, Kamima T, Adachi Y, Nakamatsu K, Monzen H. Evaluation of multiple institutions' models for knowledge-based planning of volumetric modulated arc therapy (VMAT) for prostate cancer. *Radiat Oncol*. 2018;13(1):46.
30. Loutfi-Krauss B, Kohn J, Blumer N, et al. Effect of dose reduction on image registration and image quality for cone-beam CT in radiotherapy. *Strahlenther Onkol*. 2015;191(2):192-200.